Molecular Recognition of PNA-Containing Hybrids: Spontaneous Assembly of Helical Cyanine Dye Aggregates on PNA Templates

Jeffrey O. Smith, Darren A. Olson, and Bruce A. Armitage*

Contribution from the Department of Chemistry, Carnegie Mellon University, 4400 Fifth Avenue, Pittsburgh, Pennsylvania 15213

Received October 27, 1998

Abstract: Symmetrical cyanine dyes containing benzothiazole groups have been shown to bind with high affinity to a variety of PNA-containing hybrids, including PNA/DNA duplexes, a PNA/PNA duplex, and a bisPNA/DNA triplex. Binding of a dicarbocyanine dye results in a 114 nm hypsochromic shift of the main visible absorption band. Circular dichroism spectropolarimetry reveals exciton coupling between multiple chromophores bound to the same PNA/DNA or PNA/PNA duplex, demonstrating binding of the dye as an aggregate. A continuous variations experiment indicates that the dye binds as a 6(±1):1 complex with a 12 base pair PNA/DNA duplex. The dye aggregate forms in a highly cooperative manner and exhibits a temperature-dependent self-assembly behavior which is independent of the PNA/DNA hybridization event. Experiments with mismatched and parallel duplexes demonstrate a strong preference for a continuous, antiparallel helix as a template on which to assemble the helical dye aggregate. Successful binding of the dye to the duplex and triplex indicates that dyes associate with one another in the minor groove of the template. The 114 nm shift in absorption causes an instantaneous visible color change from blue to purple, providing a convenient method for detecting PNA hybridization with its complementary target sequence.

Introduction

The most common form of nucleic acid secondary structure is the double helix, consisting of two complementary strands that recognize one another according to the Watson−Crick rules for hydrogen bond-mediated base pairing.[1,2] The double helix is the canonical structure for genetic DNA and stabilizes RNA secondary and tertiary structure through the formation of stems and pseudoknots, respectively. Due to the ubiquity of these structures, great effort has gone into the development of both natural and synthetic ligands that can recognize double helices. Protein side chains mediate recognition of double helices by interacting with the nucleic acid phosphates, by forming hydrogen bonds and/or van der Waals contacts with groups in the major and minor grooves of the nucleic acid, or by inserting residues between adjacent base pairs (intercalation).[3,4] Similar recognition mechanisms are utilized by smaller ligands of both natural and synthetic origin.[5,6] For example, ethidium bromide binds to nucleic acid double helices by intercalation, with favorable van der Waals contacts and electrostatic interactions stabilizing the complex.[7] Other ligands, such as netropsin and distamycin, recognize the minor groove of DNA at select sequences on the basis of a combination of hydrogen-bonding, van der Waals, and electrostatic interactions.[8]

Despite the great successes in designing DNA-binding ligands, similar progress has not been achieved in the recognition of other double helices, such as DNA/RNA or RNA/RNA. The inability of known DNA-binding ligands to recognize alternative duplexes with comparable affinity undoubtedly reflects the structural differences among the various types of double helices. One interesting example of this phenomenon was reported in 1994 by Nordén and co-workers, who studied the ability of DNA intercalators and minor groove binders to recognize PNA/DNA and PNA/PNA double helices.[9] (PNA is a synthetic analogue of DNA and RNA that features hydrogen-bonding nucleobases appended to a polyamide backbone.[10−14] PNA forms Watson−Crick double helices with complementary PNA,[15] DNA,[16] and

* To whom correspondence should be addressed. E-mail: army@cyrus.andrew.cmu.edu.

(1) Watson, J. D.; Crick, F. H. C. *Nature* **1953**, *171*, 737−738.
(2) Saenger, W. *Principles of Nucleic Acid Structure*; Springer-Verlag: New York, 1984.
(3) Larson, C. J.; Verdine, G. L. In *Bioorganic Chemistry: Nucleic Acids*; Hecht, S. M., Ed.; Oxford University Press: New York, 1996; pp 324−346.
(4) Glumoff, T.; Goldman, A. In *Nucleic Acids in Chemistry and Biology*, 2nd ed.; Blackburn, G. M., Gait, M. J., Eds.; Oxford University Press: Oxford, 1996; pp 375−441.
(5) Wilson, W. D. In *Nucleic Acids in Chemistry and Biology*; Blackburn, G. M., Gait, M. J., Eds.; Oxford University Press: Oxford, 1996; pp 329−374.
(6) Mountzouris, J. A.; Hurley, L. H. In *Bioorganic Chemistry: Nucleic Acids*; Hecht, S. M., Ed.; Oxford University Press: New York, 1996; ppp 288−323.
(7) LePecq, J. B.; Paoletti, C. *J. Mol. Biol.* **1967**, *27*, 87−106.
(8) Geierstanger, B. H.; Wemmer, D. E. *Annu. Rev. Biophys. Biomol. Struct.* **1995**, *24*, 463−493.
(9) Wittung, P.; Kim, S. K.; Buchardt, O.; Nielsen, P. E.; Nordén, B. *Nucleic Acids Res.* **1994**, *22*, 5371−5377.
(10) Nielsen, P. E.; Egholm, M.; Berg, R. H.; Buchardt, O. *Science* **1991**, *254*, 1498−1500.
(11) Corey, D. R. *Trends Biotechnol.* **1997**, *15*, 224−229.
(12) Erikkson, M.; Nielsen, P. E. *Q. Rev. Biophys.* **1996**, *29*, 369−394.
(13) Hyrup, B.; Nielsen, P. E. *Bioorg. Med. Chem.* **1996**, *4*, 5−23.
(14) Nielsen, P. E.; Haaima, G. *Chem. Soc. Rev.* **1997**, *26*, 73−78.
(15) Wittung, P.; Nielsen, P. E.; Buchardt, O.; Egholm, M.; Nordén, B. *Nature* **1994**, *368*, 561−563.
(16) Egholm, M.; Buchardt, O.; Christensen, L.; Behrens, C.; Freier, S. M.; Driver, D. A.; Berg, R. H.; Kim, S. K.; Nordén, B.; Nielsen, P. E. *Nature* **1993**, *365*, 566−568.

10.1021/ja9837553 CCC: $18.00
Published on Web 03/13/1999

RNA[16] strands.) Intercalators such as ethidium bromide, 8-methoxypsoralen, and ruthenium complexes with planar aromatic ligands failed to exhibit significant binding to either PNA/DNA or PNA/PNA duplexes. The minor groove binders distamycin and diamidinophenylindole (DAPI) exhibited modest affinity for PNA/DNA duplexes featuring a central AATA/TTAT sequence, but no affinity for PNA/DNA duplexes lacking the central A/T sequence. Moreover, the groove binders exhibited no affinity for any PNA/PNA duplexes. The considerably weakened interactions of the groove binders with PNA-containing hybrids was attributed to the lower negative charge density of the duplexes, leading to a weaker electrostatic attraction with the cationic ligands. (PNA is uncharged.) In addition, the significant structural differences between DNA/DNA and PNA-containing duplexes[12,17−20] likely contributes to the lower affinity by altering the hydrogen-bonding and van der Waals contact distances for the ligands and functional groups in the minor groove. Meanwhile, the inability of intercalators to bind PNA-containing hybrids remains unexplained.

The failure of traditional DNA-binding ligands to effectively recognize PNA-containing hybrids suggested the use of non-traditional ligands for PNA binding. We have been studying the binding of symmetrical cyanine dyes to duplex DNA and have found that certain compounds, such as **DiSC$_2$(5)**, prefer

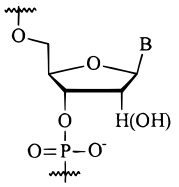

DNA (RNA)

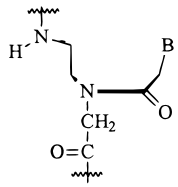

PNA

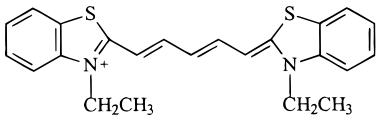

DiSC$_2$(5)

to bind within the minor groove at sequences consisting of alternating A/T pairs, such as ATATA/TATAT.[21] Moreover, the dyes insert into the minor groove as face-to-face dimers, similar to the natural ligand distamycin[22−25] and a variety of synthetic analogues.[26−28] However, unlike those compounds, there is likely to be minimal hydrogen-bonding interaction between **DiSC$_2$(5)** and the DNA due to the lack of hydrogen bond donor and acceptor groups on the dye. Instead, the binding appears to be driven primarily by hydrophobic and van der Waals interactions. Since the PNA backbone is less hydrophilic than DNA, we considered the possibility that DNA-binding cyanine dyes would also associate with PNA-containing duplexes. In this paper we describe our initial investigations, which demonstrate high-affinity binding of **DiSC$_2$(5)** to PNA/DNA, PNA/PNA, and bisPNA/DNA hybrids.

Results

Binding of a Cyanine Dye to PNA/DNA Duplexes. Symmetrical cyanine dyes generally consist of two heteroaromatic systems linked by a polymethine bridge. For example, **DiSC$_2$(5)** is constructed from two benzothiazole units connected by a pentamethine linker. The extensive conjugation in this dye yields an absorption λ_{max} of 651 nm and an extinction coefficient of 260 000 M^{-1} cm^{-1} in methanol. The intense, long-wavelength optical transitions exhibited by cyanine dyes have been exploited for a variety of applications ranging from photosensitizers for color photography[29] to probes of biomembrane fluidity.[30−38]

The hydrophobicity and polarizability of **DiSC$_2$(5)** drive noncovalent dimerization of the dye in aqueous solution.[39,40] These dimers consist of two cyanine dye molecules arranged cofacially, with the exclusion of water from the intervening medium likely playing a significant role in stabilizing the dimer. The dimeric state can be stabilized even further if a suitable binding site is introduced that will protect the exterior sides of the dimer from exposure to water. Thus, the interior of γ-cyclodextrin[41−47] and the pockets formed by the ligands of hydrophobic borate anions[48] have been shown to enhance dimerization of various dyes. Moreover, we recently discovered that **DiSC$_2$(5)** readily dimerizes within the minor groove of duplex DNA at alternating A/T sequences.[21]

(17) Brown, S. C.; Thomson, S. A.; Veal, J. M.; Davis, D. G. *Science* **1994**, *265*, 777−780.
(18) Betts, L.; Josey, J. A.; Veal, J. M.; Jordan, S. R. *Science* **1995**, *270*, 1838−1841.
(19) Erikkson, M.; Nielsen, P. E. *Nat. Struct. Biol.* **1996**, *3*, 410−413.
(20) Rasmussen, H.; Kastrup, J. S.; Nielsen, J. N.; Nielsen, J. M.; Nielsen, P. E. *Nat. Struct. Biol.* **1997**, *4*, 98−101.
(21) Seifert, J. L.; Connor, R. E.; Kushon, S. A.; Wang, M.; Armitage, B. A. *J. Am. Chem. Soc.* In press.
(22) Chen, X.; Ramakrishnan, B.; Rao, S. T.; Sundaralingam, M. *Nat. Struct. Biol.* **1994**, *1*, 169−175.
(23) Chen, X.; Ramakrishnan, B.; Sundaralingam, M. *J. Mol. Biol.* **1997**, *267*, 1157−1170.
(24) Pelton, J. G.; Wemmer, D. E. *Biochemistry* **1989**, *27*, 8088−8096.
(25) Pelton, J. G.; Wemmer, D. E. *Proc. Natl. Acad. Sci. U.S.A.* **1989**, *86*, 5723−5727.
(26) Kopka, M. L.; Goodsell, D. S.; Han, G. W.; Chiu, T. K.; Lown, J. W.; Dickerson, R. E. *Structure* **1997**, *5*, 1033−1046.
(27) Geierstanger, B. H.; Mrksich, M.; Dervan, P. B.; Wemmer, D. E. *Science* **1994**, *266*, 646−650.
(28) Dwyer, T. J.; Geierstanger, B. H.; Bathini, Y.; Lown, J. W.; Wemmer, D. E. *J. Am. Chem. Soc.* **1992**, *114*, 5911−5919.
(29) West, W.; Gilman, P. B. Spectral Sensitivity and the Mechanism of Spectral Sensitization. In *The Theory of the Photographic Process*, 4th ed.; James, T. H., Ed.; Macmillan: New York, 1977; p 277.
(30) Armitage, B.; O'Brien, D. F. *J. Am. Chem. Soc.* **1991**, *113*, 9678−9679.
(31) Armitage, B.; O'Brien, D. F. *J. Am. Chem. Soc.* **1992**, *114*, 7396−7403.
(32) Derzko, Z.; Jacobson, K. *Biochemistry* **1980**, *19*, 6050−6057.
(33) Fahey, P. F.; Koppel, D. E.; Barak, L. S.; Wolf, D. E.; Elson, E. L.; Webb, W. W. *Science* **1977**, *195*, 305−306.
(34) Fahey, P.; Webb, W. W. *Biochemistry* **1978**, *17*, 3046−3053.
(35) Klausner, R. D.; Wolf, D. E. *Biochemistry* **1980**, *19*, 6199−6203.
(36) Kurihara, K.; Toyoshima, Y.; Sukigara, M. *J. Phys. Chem.* **1977**, *81*, 1833−1837.
(37) Wolf, D. E.; Handyside, A. H.; Edidin, M. *Biophys. J.* **1982**, *38*, 295−297.
(38) Wu, E. S.; Jacobson, K.; Papahadjopoulos, D. *Biochemistry* **1977**, *16*, 3936−3941.
(39) West, W.; Pearce, S. *J. Phys. Chem.* **1965**, *69*, 1894−1903.
(40) Herz, A. H. *Photogr. Sci. Eng.* **1974**, *18*, 323−335.
(41) Kasatani, K.; Ohashi, M.; Kawasaki, M.; Sato, H. *Chem. Lett.* **1987**, 1633−1636.
(42) Wenzel, S.; Brinschwitz, T.; Lenzmann, F.; Buss, V. *J. Inclusion Phenom. Mol. Recognit. Chem.* **1995**, *22*, 277−284.
(43) Roos, C.; Buss, V. *J. Inclusion Phenom. Mol. Recognit. Chem.* **1997**, *27*, 49−56.
(44) Kasatani, K.; Ohashi, M.; Sato, H. *Carbohydr. Res.* **1989**, *192*, 197−214.
(45) Buss, V. *Minutes, Sixth International Symposium on Cyclodextrins*, Chicago, 1992; pp 160−165.
(46) Ohashi, M.; Kasatani, K.; Shinohara, H.; Sato, H. *J. Am. Chem. Soc.* **1990**, *112*, 5824−5830.
(47) Buss, V. *Angew. Chem., Int. Ed. Engl.* **1991**, *30*, 869−870.
(48) Armitage, B.; Retterer, J.; O'Brien, D. F. *J. Am. Chem. Soc.* **1993**, *115*, 10786−10790.

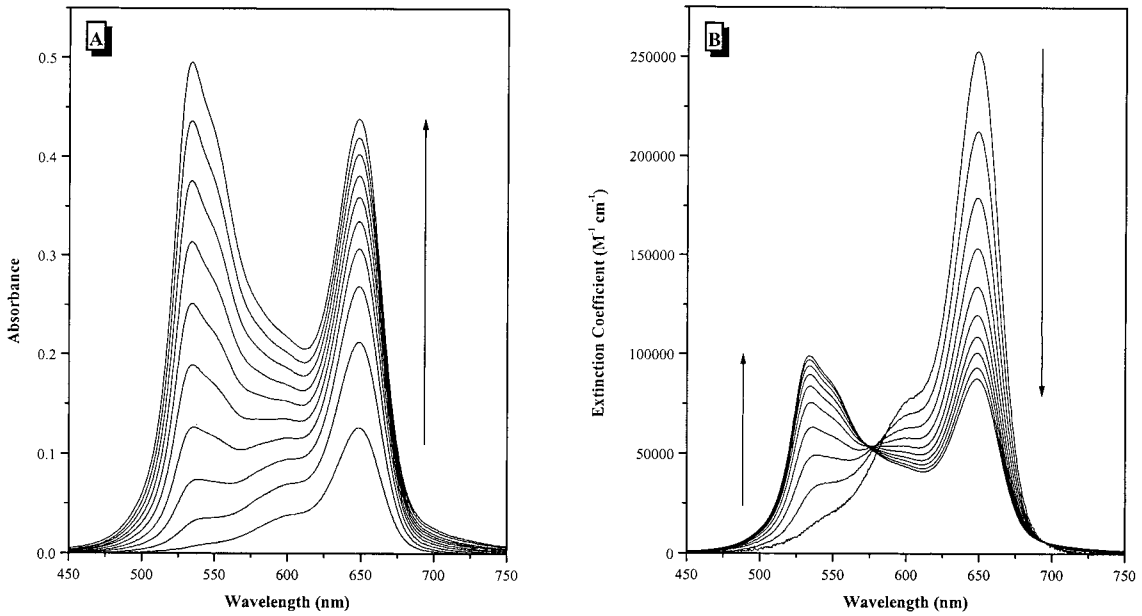

Figure 1. UV−vis titration of **PD1** with **DiSC$_2$(5)**. [**PD1**] = 5.0 μM; dye added in 0.5 μM aliquots. Spectra were recorded at 15 °C. (A) Absorbance spectra. (B) Extinction coefficient spectra, obtained by dividing the absorbance spectra from (A) by the corresponding dye concentration.

Thermodynamic data[49,50] and molecular dynamics simulations[51] indicate that PNA-containing hybrids are significantly more hydrophobic than their corresponding all-DNA analogues. Thus, the stabilizing interactions involved in binding dimeric **DiSC$_2$(5)** within γ-cyclodextrin or the minor groove of DNA could also permit binding of the dye to PNA/DNA duplexes. Figure 1 illustrates the effect of titrating a solution of **DiSC$_2$(5)** into a solution containing 5.0 μM **PD1**. At low dye concentrations, the absorption spectrum is similar to that recorded for the dye dissolved in methanol, with λ_{max} = 648 nm. However, as the dye concentration increases, a new peak appears at 534 nm. Figure 1B, which plots the apparent extinction coefficient versus wavelength, illustrates how the growth of the new band comes at the expense of the 648 nm band. The 534 nm absorption band is not observed if the dye is added to solutions containing (i) single-stranded (ss) PNA, (ii) ss DNA, or (iii) double-stranded (ds) DNA identical in sequence to **PD1**. These control experiments demonstrate that the 114 nm hypsochromic shift of λ_{max} is due to binding of the dye to the PNA/DNA duplex.

We should point out that **PD1** is the same sequence to which traditional DNA intercalators and minor groove binders exhibited no binding.[9] Thus, **DiSC$_2$(5)** not only represents the first high-affinity ligand for PNA/DNA duplexes, but readily binds to sequences that contain mixtures of purines and pyrimidines on both strands. Similar results have been found for other mixed sequence PNA/DNA hybrids (Chart 1), demonstrating the generality of this recognition event.

Binding Stoichiometry. DiSC$_2$(5) exhibits modest solvatochromism: Table 1 lists the observed λ_{max} values for the dye recorded in a range of solvents. It is clear from these data that, as the solvent dielectric constant decreases, λ_{max} shifts to the *red*. Binding of the dye to PNA/DNA likely places the dye in a lower dielectric constant environment than water, yet λ_{max} shifts by 114 nm to the *blue*. This result argues against binding of the dye as a monomer.

Chart 1. Sequences of PNA-Containing Hybrids

PD1	H-AGT-GAT-CTA-C-Lys-NH_2 3'-TCA-CTA-GAT-G-5'	**PD3**	H-GAT-CAT-CAT-CG-Lys-NH_2 3'-CTA-GTA-GTA-GC-5'
PD2	H-CCG-TAT-CGC-CCG-NH_2 3'-GGC-ATA-GCG-GGC-5'	**PDP1**	H-TJTJTTT 3'-AGAGAAA-5' H_2N-Lys-TCTCTTT
PD2m	H-CCG-TAT-CGC-CCG-NH_2 3'-GGC-ATA-CCG-GGC-5'		
PD2p	H-CCG-TAT-CGC-CCG-NH_2 5'-GGC-ATA-GCG-GGC-3'	**PP1**	H-AGT-GAT-CTA-C-Lys-NH_2 H_2N-Lys-TCA-CTA-GAT-G-H

Table 1. Solvatochromism of **DiSC$_2$(5)**

solvent (dielectric constant)	λ_{max} (nm)	solvent (dielectric constant)	λ_{max} (nm)
water (78.5)	646	ethyl acetate (6.0)	658
acetonitrile (38.8)	650	benzene (2.3)	680
methanol (32.6)	651	water[a]	579
acetone (20.7)	653	γ-cyclodextrin[a]	580
ethanol (24.3)	655	DNA[a]	590
2-propanol (18.3)	656	PNA/DNA	534

[a] Under conditions where **DiSC$_2$(5)** dimerizes.

Dimerization of **DiSC$_2$(5)** in aqueous solution results in a ca. 70 nm hypsochromic shift of the absorption band to 579 nm.[19] Dimers formed within the central cavity of γ-cyclodextrin[13] absorb maximally at 580 nm, while dimers bound within the minor groove of DNA absorb at 590 nm.[21] Thus, whether dissolved in water, surrounded by a cyclic oligosaccharide, or bound to DNA, dimeric **DiSC$_2$(5)** exhibits similar λ_{max} values. It is highly unlikely that binding of dimeric **DiSC$_2$(5)** to a PNA/DNA duplex would shift λ_{max} by an additional ca. 45−55 nm. However, the 534 nm absorption band could be rationalized if the dye were to bind as a higher aggregate.

Further evidence for multimeric binding of **DiSC$_2$(5)** to **PD1** is obtained from circular dichroism (CD) spectropolarimetry. Association of the dye with the right-handed PNA/DNA double helix relieves the symmetry of the dye structure and induces circular dichroism in the 534 nm absorption band of the dye. Figure 2 demonstrates the induced CD spectra collected as a function of dye concentration. Increasing dye concentration results in a positive CD signal at 558 nm and a negative signal

(49) Ratilainen, T.; Holmén, A.; Tuite, E.; Haaima, G.; Christensen, L.; Nielsen, P. E.; Nordén, B. *Biochemistry* **1998**, *37*, 12331−12342.
(50) Tomac, S.; Sarkar, M.; Ratilainen, T.; Wittung, P.; Nielsen, P. E.; Nordén, B.; Gräslund, A. *J. Am. Chem. Soc.* **1996**, *118*, 5544−5552.
(51) Sen, S.; Nilsson, L. *J. Am. Chem. Soc.* **1998**, *120*, 619−631.

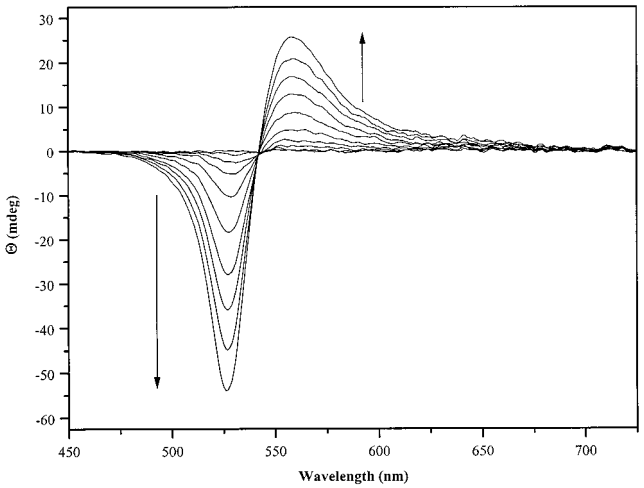

Figure 2. CD titration of **PD1** with **DiSC$_2$(5)**. [**PD1**] = 5.0 μM; dye added in 0.5 μM aliquots. Spectra were recorded at 15 °C, and either two or four scans collected at 200 nm/min were averaged.

at 529 nm. An isoelliptic point is observed at 544 nm, except for the first two spectra.

The bisignate bands observed in Figure 2 are attributed to exciton coupling among multiple **DiSC$_2$(5)** molecules.[52] Exciton coupling is favored when the individual chromophores have large extinction coefficients and/or are positioned close to one another.[53] Thus, the observed exciton coupling in this experiment indicates that multiple dye molecules are simultaneously bound to the PNA/DNA duplex. Since the ratio of **DiSC$_2$(5)**:**PD1** $\leq$ 1.0 throughout the titration, cyanine dye binding to the duplex must be cooperative. This is consistent with the UV−vis data that indicated binding of the dye as a higher aggregate. It is also noteworthy that the shape of the induced CD spectrum is invariant once the ratio of dye:duplex exceeds 0.2, indicating that there is a single CD-active species bound to the PNA/DNA duplex above this ratio.

Binding stoichiometries can be determined by the method of continuous variations, in which the individual components are mixed in variable ratios, but constant total concentration.[54] A plot of some experimental observable versus the mole fraction (X) of one of the components will exhibit an inflection at the X value corresponding to the binding stoichiometry. If multiple complexes (e.g., 1:1, 2:1, etc.) are formed, then inflections may be observed corresponding to each stoichiometry. Figure 3 illustrates how the absorbance at 534 nm varies with the mole fraction of **DiSC$_2$(5)** relative to **PD2**. The absorbance increases progressively with the mole fraction of dye (X_{Dye}) and only begins to decrease in the vicinity of $X_{\mathrm{Dye}} = 0.85$. While this value corresponds most closely to a 6:1 stoichiometry ($X_{\mathrm{Dye}} = 0.857$), 5:1 ($X_{\mathrm{Dye}} = 0.833$) and 7:1 ($X_{\mathrm{Dye}} = 0.875$) complexes cannot be ruled out due to the lack of a sharp inflection in the plot. The important point to be made about the data in Figure 3 is that a higher aggregate of the dye is indeed formed on the duplex and that assembly of the aggregate is a highly cooperative process. (The lack of an inflection at $X_{\mathrm{Dye}} = 0.50$ (1:1) or 0.67 (2:1) verifies that the dye does not bind to the duplex as either a monomer or a dimer.)

(52) Nakanishi, K.; Berova, N.; Woody, R. W. *Circular Dichroism: Principles and Applications*; VCH Publishers: New York, 1994.

(53) Rodger, A.; Nordén, B. *Circular Dichroism and Linear Dichroism*; Oxford University Press: Oxford, 1997; Vol. 1.

(54) Job, P. *Ann. Chim. (Paris)* **1928**, *9*, 113−203.

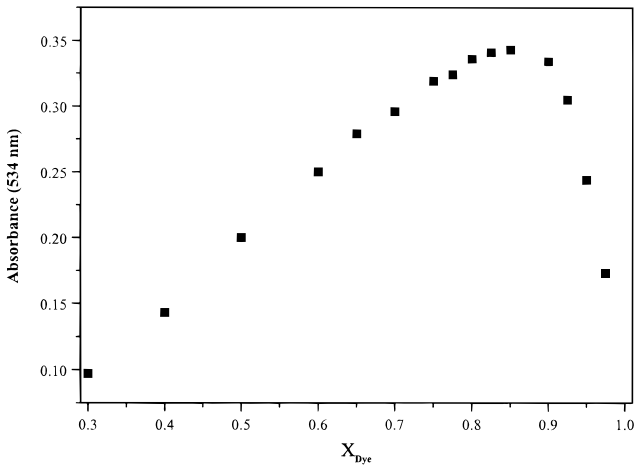

Figure 3. Continuous variations experiment to determine **DiSC$_2$(5)**:[**PD2**] binding stoichiometry. [**DiSC$_2$(5)**] + [**PD2**] = 5.0 μM throughout the experiment. Spectra were recorded at 15 °C.

Chart 2. Other Cyanine Dyes

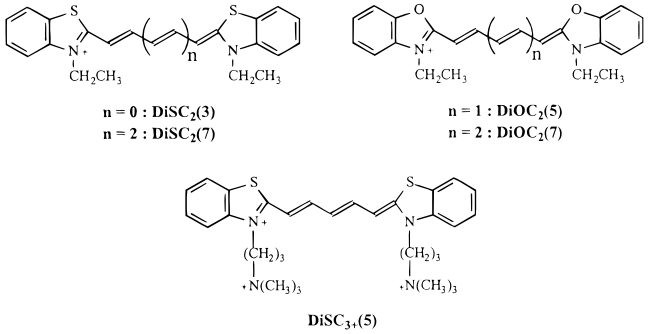

The spectral data shown in Figure 1 can be used to estimate a binding constant (K_{B}) on the basis of discrete binding of the dye as a 6:1 complex (eq 1) where $(\mathrm{Cy})_6\cdots\mathrm{PD}$ represents a

$$K_{\mathrm{B}} = \frac{[(\mathrm{Cy})_6\cdots\mathrm{PD}]}{[\mathrm{Cy_f}]^6[\mathrm{PD_f}]} \qquad (1)$$

DiSC$_2$(5) hexamer bound to a PNA/DNA duplex while $\mathrm{Cy_f}$ and $\mathrm{PD_f}$ represent free **DiSC$_2$(5)** and duplex, respectively. As described in the Appendix, extinction coefficients for the free and bound dye can be estimated from the spectral data and used to calculate the free and bound dye concentrations using the Beer−Lambert law. These calculations yield an equilibrium constant of $K_{\mathrm{B}} = 1.6 \times 10^{35}$ M^{-6} for binding of a hexameric aggregate of **DiSC$_2$(5)** to **PD1**.[55]

Binding of Other Cyanine Dyes to PNA/DNA Duplexes. The general cyanine dye structure can be subdivided into three features: (i) the heterocyclic units, (ii) the *N*-substituents, and (iii) the polymethine bridge. We studied analogues of **DiSC$_2$(5)** to understand which features of the dye contribute most to the PNA-recognition capabilities (Chart 2). **DiOC$_2$(5)** substitutes benzoxazole for benzothiazole rings. This dye exhibited very weak binding to **PD2** on the basis of a slight attenuation of the absorption intensity at λ_{max} (575 nm) and the appearance of a shoulder on the short-wavelength side of the spectrum (Figure S1, Supporting Information). This result demonstrates the critical need for the benzothiazole groups in **DiSC$_2$(5)**.

(55) The corresponding values for 5:1 and 7:1 complexes are $K_{\mathrm{B}} = 1.9 \times 10^{29}$ M^{-5} and 1.3×10^{41} M^{-7}, respectively.

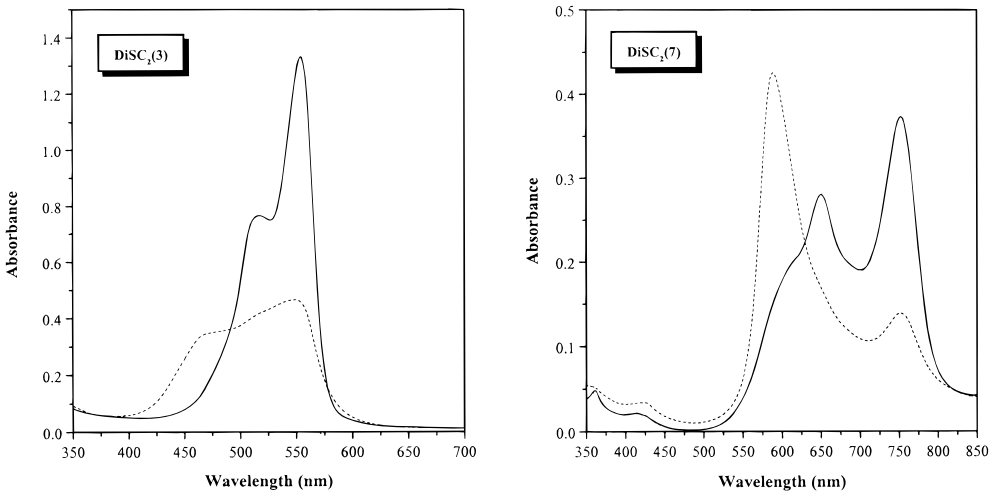

Figure 4. Effect of **PD2** on UV−vis absorption spectra recorded for benzothiazole cyanine dyes. [**PD2**] = 5.0 μM, [**DiSC$_2$(3)**] = 10 μM, and [**DiSC$_2$(7)**] = 5.0 μM. Spectra were recorded at 15 °C. The buffer contained 10 mM NaP_i (pH 7.0), 100 mM NaCl, and 10% methanol. Solid line: buffer alone. dashed line: with **PD2**.

DiSC$_{3+}$(5) retains the heterocyclic groups and pentamethine bridge of **DiSC$_2$(5)**, but possesses cationic side chains. This gives the dye a charge of +3 as opposed to +1 for the parent compound. UV−vis analysis exhibited virtually no change in the spectral profile and intensity in the presence of **PD2**, indicating that the dye does not bind to the duplex (data not shown). Presumably, the lower hydrophobicity and greater electrostatic repulsions between dye molecules inhibit formation of a PNA/DNA-bound aggregate for the tricationic dye.

The tendency of cyanine dyes to aggregate in water increases with the length of the polymethine bridge linking the two heterocyclic units.[39] This effect is also observed in aggregation of the dyes on PNA/DNA. Extension of the bridge by two carbons for the benzoxazole dye (i.e., **DiOC$_2$(7)**) leads to enhanced binding, on the basis of a greater attenuation of the peak intensity and the growth of a distinct shoulder relative to **DiOC$_2$(5)** (Figure S1, Supporting Information).

A more dramatic effect is observed for variation of the polymethine bridge length for benzothiazole dyes (Figure 4). The trimethine dye, **DiSC$_2$(3)**, readily binds to **PD2** on the basis of its attenuated and broadened absorption spectrum. The lack of a sharp new absorption band in the presence of the duplex suggests that the dye does not aggregate into a well-defined structure, in contrast to **DiSC$_2$(5)**. The heptamethine dye **DiSC$_2$(7)** also binds to **PD2**, with the growth of a new band at 588 nm. (The avid aggregation of this dye even in the absence of the duplex is apparent in the absorption spectrum.) The shift in the absorption maximum upon binding of **DiSC$_2$(7)** to **PD2** is 164 nm.

Collectively, these results demonstrate how structural variations that increase hydrophobicity promote aggregation of cyanine dyes on PNA/DNA duplexes. Moreover, the tendency of cyanine dyes to aggregate in water appears to be a useful indicator of their ability to aggregate on PNA/DNA. However, this correlation will not necessarily apply to other aggregating dyes, particularly more rigid compounds, since it is likely that the flexibility of the polymethine bridge promotes aggregation of the cyanine dyes on PNA/DNA by allowing the aggregate to twist in phase with the helical duplex template.

Thermal Analysis. Binding of a ligand to duplex DNA generally leads to increased thermal stability of the duplex, provided the ligand has higher affinity for the duplex than for the single strands. Given the observation that the 534 nm band was not observed in the presence of either ss PNA or ss DNA,

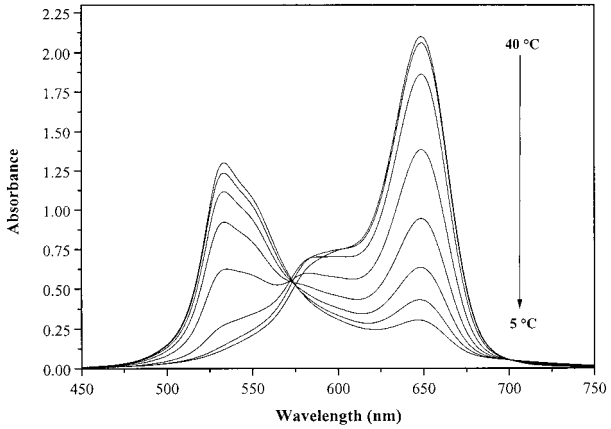

Figure 5. Variable temperature UV−vis spectra. [**PD1**] = 5.0 μM, and [**DiSC$_2$(5)**] = 10 μM. Spectra were recorded at 5 °C intervals ranging from 40 to 5 °C.

it seemed reasonable to expect that **DiSC$_2$(5)** would stabilize **PD1** against thermal denaturation. To test this prediction, we measured the temperature-dependent UV absorbance at 260 nm to determine the thermal denaturation temperature (T_m) of **PD1** in the absence and presence of **DiSC$_2$(5)**. Surprisingly, a single melting transition was observed with precisely the same T_m (49 °C) in both cases. Thus, while the dye clearly binds to the duplex with high cooperativity and affinity, it has no effect on the thermal stability of the duplex.

To gain insight into why **DiSC$_2$(5)** failed to stabilize the PNA/DNA duplex, we measured UV−vis absorption spectra of the dye as a function of temperature (Figure 5). At 40 °C, the spectrum is identical to that recorded in the absence of **PD1**, demonstrating that the dye is completely unbound at a temperature that is nearly 10 °C lower than the melting temperature of the duplex (T_m = 49 °C). As the temperature is decreased to 35 and 30 °C, a slight decrease in absorbance at 648 nm is detected and a shoulder appears in the 530−540 nm range. As the temperature is decreased further, the intensity at 648 nm decreases sharply while the 534 nm band appears. In the range 25−0 °C, a clean isosbestic point is observed at 573 nm.

The abruptness of the dye binding as the sample is cooled is evident in Figure 6, which shows the temperature-dependent changes in absorbance at 260, 534, and 648 nm for 5.0 μM **PD1** and 10 μM **DiSC$_2$(5)**. The data recorded at 260 nm reveal

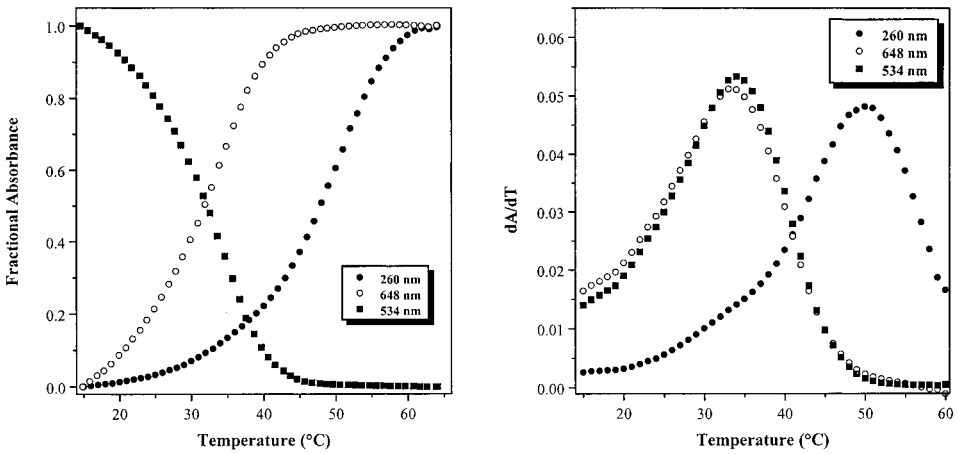

Figure 6. Temperature-dependent absorbance and first-derivative (d*A*/d*T*) curves recorded at 260, 534, and 648 nm. [**PD1**] = 5.0 μM, and [**DiSC$_2$-(5)**] = 10 μM. Cooling curves were collected from 65 to 0 °C at a rate of 0.5 °C/min.

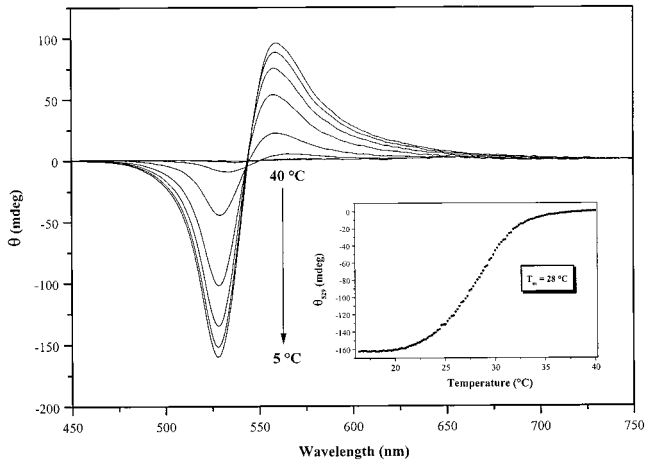

Figure 7. Variable temperature CD spectra. [**PD1**] = 5.0 μM, and [**DiSC$_2$(5)**] = 10 μM. Spectra were recorded at 5 °C intervals ranging from 40 to 5 °C. Inset: CD signal recorded at 529 nm as a function of temperature as the sample was cooled from 40 to 15 °C at a rate of 0.5 °C/min.

a transition at 49 °C, attributed to the T_m for the PNA/DNA duplex. The data recorded at the two visible wavelengths each give transitions at 27 °C and reflect the binding of the dye. This transition is highly dependent on the concentration of **DiSC$_2$(5)**: at 5.0 μM dye, the transition recorded at the visible wavelengths decreases by 7 °C to 20 °C, a manifestation of the cooperativity inherent in binding of **DiSC$_2$(5)** to **PD1**.

Temperature-dependent CD measurements are consistent with the UV−vis data shown in Figures 5 and 6. As a sample containing 10 μM **DiSC$_2$(5)** and 5.0 μM **PD1** is cooled, the exciton feature appears at 30 °C and becomes more intense with decreasing temperature (Figure 7). A cooling curve recorded by monitoring the CD intensity at 529 nm yielded a transition at 28 °C (inset). Thus, the transition detected by the absorbances at 534 and 648 nm is correlated with induction of chirality due to binding of **DiSC$_2$(5)** to the PNA/DNA duplex.

Effect of Single Base Mismatches. Binding of **DiSC$_2$(5)** to an imperfect PNA/DNA hybrid was investigated by comparing **PD2** with **PD2m**, which possesses a C−C mismatch near the center of the duplex (Chart 1). This mismatch destabilizes the duplex by 19 °C; nevertheless, the mismatched duplex (T_m = 46.1 °C) forms a stable hybrid at room temperature.

Binding of 5.0 μM dye to the fully matched duplex occurs with a transition at 29.9 °C. However, introduction of a single mismatch near the center of the duplex causes the dye T_m to decrease to 26.4 °C. (See Figure S2, Supporting Information.) This effect cannot be attributed to the stability of the duplex, which is fully formed in both cases at temperatures below 35 °C. Instead, the lower affinity of the dye for the hybrid is likely due to the structural perturbation introduced by the mismatched pair. Thus, a continuous double helix is essential for optimal binding of the dye.

Binding of DiSC$_2$(5) to Other PNA-Containing Hybrids. PNA/PNA Duplex. Complementary strands of PNA hybridize to form stable double-helical complexes.[15] The lack of a negative charge on the PNA backbone means that a PNA/PNA duplex bears a net positive charge. For example, **PP1** has the same sequence as **PD1**, but both strands have the PNA backbone, so the net charge is +4 due to the C-terminal lysine side chains and the protonated amino groups at the N-termini. This contrasts with **PD1**, where the nine phosphate groups on the DNA strand provide a net negative charge to the duplex.

Figure 8 shows the absorbance and CD spectra recorded for **DiSC$_2$(5)** in the presence of **PP1**. The absorbance spectrum recorded at 45 °C shows little evidence of binding by the dye. However, cooling to 15 °C causes a new band to appear at 535 nm, similar to what is observed in the presence of **PD1**. Thermal analysis reveals that the dye T_m on **PP1** is 7−8 °C *higher* than for binding to **PD1** (see Table 2). This result demonstrates that the dye has greater affinity for PNA/PNA than PNA/DNA and indicates that electrostatics are of minor importance in binding of the cationic dye to the duplex.

One additional observation worth noting is the shape of the induced CD spectrum for the dye when bound to **PP1**: the exciton band is inverted relative to **PD1**. PNA/DNA duplexes exhibit right-handed helicities, due in large part to the inherent chirality of the DNA strand. The PNA backbone is achiral; however, PNA/PNA duplexes with C-terminal L-lysine residues are chiral and, therefore, exhibit CD spectra.[15,56] Initial studies performed on the chiral **PP1** duplex indicated that a right-handed helical orientation was preferred, on the basis of similarity in the shape of its CD spectrum with that observed for B-form DNA.[15,56] However, more recent data suggest that the preferred orientation of PNA/PNA duplexes with L-lysine residues at the C-termini is left-handed.[57] Our data are consistent with this latter interpretation: the mirror-image relationship between the CD spectra for **DiSC$_2$(5)** bound to **PD1** versus **PP1** likely arises

(56) Wittung, P.; Erikkson, M.; Lyng, R.; Nielsen, P. E.; Nordén, B. *J. Am. Chem. Soc.* **1995**, *117*, 10167−10173.
(57) Lagriffoule, P.; Wittung, P.; Erikkson, M.; Jensen, K. K.; Nordén, B.; Buchardt, O.; Nielsen, P. E. *Chem. Eur. J.* **1997**, *3*, 912−919.

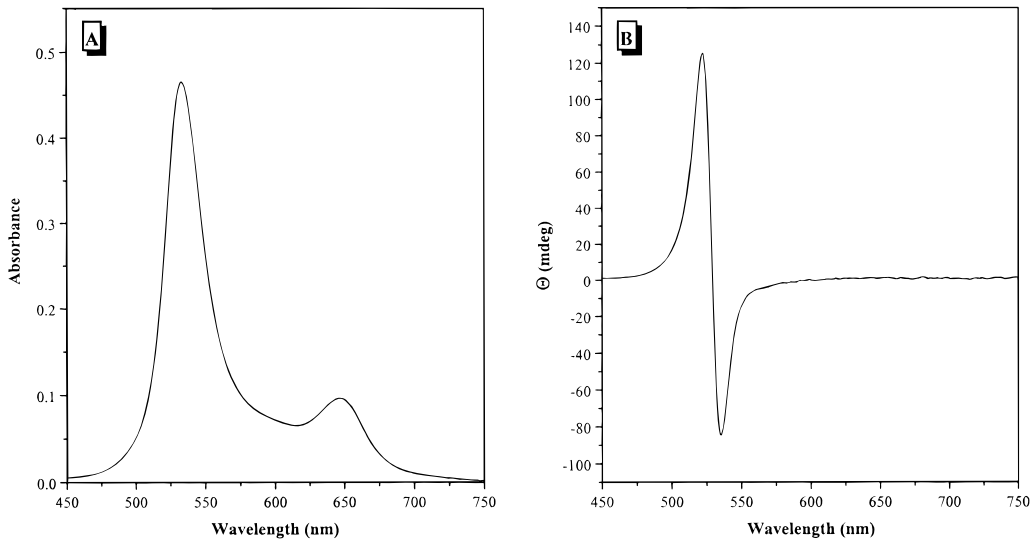

Figure 8. UV−vis absorbance and CD spectra recorded for **DiSC$_2$(5)** bound to a PNA/PNA duplex. [**PP1**] = 2.0 μM, and [**DiSC$_2$(5)**] = 5.0 μM. The buffer contained 10 mM NaP_i (pH 7.0), 100 mM NaCl, and 10% methanol. Spectra were recorded at 15 °C.

Table 2. Comparison of the Temperature Dependence of **DiSC$_2$(5)** Binding to PNA-Containing Hybrids[a]

hybrid	hybrid T_m (°C)	dye T_m (°C)
PD1	49	20
PP1	67	28
PDP1	61	24

[a] 5.0 μM **DiSC$_2$(5)**, 5.0 μM hybrid, 10 mM NaP_i (pH 7.0), 100 mM NaCl, 20% methanol.

from opposite twists for the two helices: right-handed for **PD1** and left-handed for **PP1**. Thus, while the cyanine dye spontaneously assembles into a helical aggregate in both cases, the dye helix twists in opposite directions on the basis of the helical twist of the duplex "template" on which it forms.

BisPNA/DNA Triplex. Binding of **DiSC$_2$(5)** to a bisPNA/DNA triplex was studied. A bisPNA consists of two homopyrimidine "arms" joined by a flexible linker.[58,59] The two homopyrimidine sequences can simultaneously bind to a homopurine DNA sequence, with one arm forming Watson−Crick base pairs and the second arm forming Hoogsteen base pairs.[18] The triplex **PDP1**, consisting of seven base triplets, readily binds the dye on the basis of UV−vis spectra (data not shown). **DiSC$_2$(5)** bound to **PDP1** exhibits a T_m that is intermediate between those of **PD1** and **PP1** (Table 2).

Parallel PNA/DNA Duplex. PNA is capable of forming both parallel and antiparallel duplexes with DNA, albeit with lower thermal stability for the former.[16] In the parallel orientation, the PNA N-terminus is aligned with the DNA 5′-terminus. CD measurements[16] and molecular dynamics simulations[51] indicate that the duplex structures are significantly different for the two orientations.

PD2 and **PD2p** are, respectively, antiparallel and parallel 12 base pair PNA/DNA duplexes (Chart 1). The melting temperatures for these two hybrids are 66 and 51 °C, so stable duplexes will be formed in both cases at temperatures significantly higher than the dye T_m, thereby permitting a meaningful assessment of whether **DiSC$_2$(5)** can discriminate between the two orientations.

Figure 9 illustrates the temperature-dependent absorbance at 534 nm of samples containing 5.0 μM PNA/DNA duplex and 10 μM **DiSC$_2$(5)**. The dye T_m for the antiparallel duplex occurs at 25 °C, compared with 5.5 °C for the parallel duplex. Since the two duplexes are completely formed at the temperatures where the dyes begin to bind, the difference in thermal stability of the dye/hybrid complexes must be due to the different structures of the antiparallel and parallel duplexes.

Colorimetric Detection of PNA-Containing Hybrids. Binding of the dye to PNA is revealed even before the UV−vis spectrum is acquired, since the shift of the absorption λ_{max} from 648 to 534 nm results in an instantaneous visible color change from blue to purple. This effect is demonstrated in a microtiter plate format in Figure 10. Well 1 contains 15 μM **DiSC$_2$(5)** in buffer, while wells 2 and 3 contain the same concentration of dye in the presence of 600 pmol (3.0 μM) of either DNA or PNA, respectively. Well 2 shows that there is some binding of the dye to the ss DNA, since the color changes to a different shade of blue. Wells 4−7 contain the dye, PNA, and increasing amounts (150−600 pmol; 0.75−3.0 μM) of complementary DNA. The development of the purple color as the complementary DNA concentration increases is evident. Well 8 shows that if the PNA and DNA strands are noncomplementary, the purple color does not appear. Instead, the color looks like it did in the presence of only ss DNA (well 2).

Discussion

Binding of **DiSC$_2$(*n*)** (***n*** = 3, 5, or 7) to **PD1**, **PD2**, **PD3**, and **PP1** represents the first example of ligand binding to mixed sequence PNA-containing hybrids. The failure to observe high-affinity binding of either DNA intercalators or minor groove binders to mixed sequence PNA/DNA and PNA/PNA duplexes[9] naturally raises the question of how the cyanine dyes are able to recognize these structures. Four potential binding modes are considered: (i) intercalation, (ii) exterior stacking, (iii) major groove binding, and (iv) minor groove binding. The UV−vis and CD spectral data provide strong evidence for binding of **DiSC$_2$(5)** in an aggregated state, while the continuous variations experiment and thermal analysis revealed that the dye aggregate forms in a highly cooperative process. This likely rules out an intercalative binding mode since multiple dye molecules should be unable to simultaneously bind at a single intercalation site.

(58) Griffith, M. C.; Risen, L. M.; Greig, M. J.; Lesnik, E. A.; Sprankle, K. G.; Griffey, R. H.; Kiely, J. S.; Freier, S. M. *J. Am. Chem. Soc.* **1995**, *117*, 831−832.

(59) Egholm, M.; Christensen, L.; Dueholm, K. L.; Buchardt, O.; Coull, J.; Nielsen, P. E. *Nucleic Acids Res.* **1995**, *23*, 217−222.

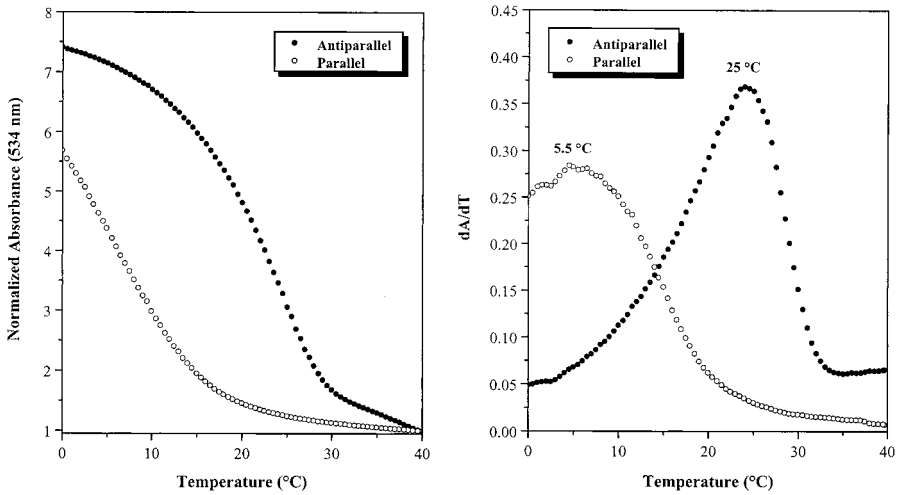

Figure 9. Temperature-dependent absorbance curves recorded at 534 nm for **DiSC$_2$(5)** (10 μM) in the presence of either **PD2** or **PD2p** (5.0 μM). Cooling curves were collected from 40 to 0 °C at a rate of 0.5 °C/min. (A) Fractional absorbance versus temperature curves. (B) First-derivative curves.

Figure 10. PNA/DNA hybridization induces a blue−purple color change: well 1, no PNA or DNA; well 2, 600 pmol (3.0 μM) of DNA; wells 3−7, 600 pmol of PNA + 0, 150, 300, 450, and 600 pmol of complementary DNA; well 8, 600 pmol of PNA + 600 pmol of noncomplementary DNA. The complementary PNA + DNA strands formed the hybrid **PD2** (Chart 1), while the noncomplementary DNA strand used in well 8 had the sequence 5′-CGATGATGATC-3′. All samples contained 15 μM **DiSC$_2$(5)**.

Certain cationic porphyrins have been proposed to bind to duplex DNA via an exterior stacking mode.[60−63] This binding mode is stabilized by electrostatic attractions between the cationic porphyrins and the anionic phosphate groups. The partial charge neutralization permits individual porphyrins to stack on top of one another, forming a helical columnar aggregate. A similar binding mode for **DiSC$_2$(5)** to the PNA-containing hybrids studied here is unlikely given the observation that the dye associates similarly with PNA/DNA and PNA/PNA duplexes having identical sequences. In fact, the T_m for the dye bound to PNA/PNA is significantly higher than for PNA/DNA (Table 2), indicating that electrostatics contribute little to the binding affinity. Instead, favorable van der Waals interactions within the dye aggregate and between the aggregate and the hybrid are probably more important in stabilizing the complex.

Recognition within the major groove could account for the ability of **DiSC$_2$(5)** to bind PNA/DNA when traditional DNA intercalators and minor groove binders fail to bind. However, the ability of the dye to bind to a bisPNA/DNA triplex in a manner similar to that observed for PNA/DNA and PNA/PNA duplexes argues against this type of binding, since the major groove is occupied by the Hoogsteen arm of the bisPNA.

High-resolution structures have been determined by NMR methods for a PNA/DNA duplex[19] and by X-ray crystallography for a bisPNA/DNA triplex[18] as well as for a PNA/PNA duplex.[20] The structures exhibit differing helical repeats: 13 base pairs for the PNA/DNA duplex, 16 base triplets for the bisPNA/DNA triplex, and 18 base pairs for the PNA/PNA duplex. However, the three structures feature similar minor groove widths, ca. 10 Å in each case.

A possible minor groove binding mode for **DiSC$_2$(5)** to the PNA-containing hybrids was investigated by comparing association of the dye with parallel and antiparallel PNA/DNA duplexes. A high-resolution structure of a parallel duplex has not been determined by experimental methods. However, a molecular dynamics simulation yielded a structure in which the minor groove width was 12.4 Å, compared with 10.2 Å for the antiparallel duplex of the same sequence.[51] **DiSC$_2$(5)** readily binds to the **PD2** antiparallel duplex (Figure 9). However, binding of the dye to the parallel duplex **PD2p** requires cooling to a significantly lower temperature. Taken together, these results suggest that the minor grooves of PNA/PNA, PNA/DNA/PNA,

(60) Pasternack, R. F.; Giannetto, A.; Pagano, P.; Gibbs, E. J. *J. Am. Chem. Soc.* **1991**, *113*, 7799−7800.
(61) Mukundan, N. E.; Pethö, G.; Dixon, D. W.; Kim, M. S.; Marzilli, L. G. *Inorg. Chem.* **1994**, *33*, 4676−4687.
(62) Mukundan, N. E.; Pethö, G.; Dixon, D. W.; Marzilli, L. G. *Inorg. Chem.* **1995**, *34*, 3677−3687.
(63) Hudson, B. P.; Sou, J.; Berger, D. J.; McMillin, D. R. *J. Am. Chem. Soc.* **1992**, *114*, 8997−9002.

and antiparallel PNA/DNA hybrids provide suitable binding sites for **DiSC$_2$(5)**, but that the parallel PNA/DNA duplex minor groove is apparently too wide to promote assembly of the dye aggregate.

An interesting comparison can be made between DNA and PNA recognition by **DiSC$_2$(5)**. The dye binds to alternating A/T sequences in duplex DNA by inserting into the minor groove as a face-to-face dimer.[21] Because the minor groove must widen to accommodate ligands in this manner, the binding of additional dimers in an end-to-end fashion is highly cooperative. For extended sequences, this leads to assembly of helical aggregates of cyanine dye dimers inserted into the minor groove. However, this binding mode is only observed for alternating A/T sequences.

DiSC$_2$(5) also binds to PNA-containing hybrids by forming helical aggregates. As described above, these aggregates also appear to use the minor groove as the template on which to assemble. However, we do not believe that the dye molecules insert deeply into the minor groove on the basis of the ability of the dye aggregates to assemble on mixed sequence hybrids. This is in contrast to DNA minor groove binders, which normally exhibit very low affinity for mixed sequences.[8] Experiments are currently underway to systematically analyze the sequence dependence of cyanine dye aggregation on PNA templates.

On the basis of the extent of the hypsochromic shift observed in the absorption spectrum, it is likely that the aggregate consists of face-to-face interactions between individual dye monomers assembled into at least a trimeric unit.[64] Cooperative, end-to-end interactions between adjacent trimers could then account for formation of higher aggregates, as indicated by the Job plot. However, as noted above, we cannot rule out alternative stoichiometries, such as 5:1 or 7:1 complexes. Nevertheless, the ca. 10 Å wide minor groove for antiparallel PNA/DNA matches well with a trimer in which the three **DiSC$_2$(5)** molecules are associated with one another cofacially. This model also suggests an explanation for the inhibited binding to parallel PNA/DNA: if the MD simulations[51] accurately reproduce the solution structure, then this duplex would have to narrow its minor groove by approximately 2.0 Å to optimally bind the trimeric dye. Alternatively, a **DiSC$_2$(5)** tetramer might be expected to bind to the minor groove of the parallel duplex. However, this would likely require a significantly lower temperature or higher dye concentration than is needed for formation of the trimer. Ultimately, definition of the binding stoichiometry and structure will require high-resolution analysis.

Finally, the instantaneous visible color change forms the basis for a convenient method for detecting PNA/DNA hybridization. While the assay lacks the sensitivity of the elegant method recently reported by Mirkin, Letsinger, and co-workers using gold nanoparticles as the basis for colorimetric detection of DNA sequences,[65−67] the cyanine dye could be a useful reagent for reporting on successful binding of PNA to its target sequence. For example, we are currently exploring the restrictions imposed by target secondary and tertiary structure on PNA hybridization, an issue of fundamental concern in the development of PNA as an antisense agent. Successful hybridization can be assayed in many formats, such as gel-mobility shift analysis or circular dichroism. However, hybridization in the presence of the cyanine dye is immediately revealed by the purple color of the solution. Our efforts in this direction will be reported shortly.

Future Work. Thermodynamic and structural analysis of the cyanine dye binding to the PNA-containing hybrids in Chart 1 will be complicated by the multiple potential binding sites for the dye on the hybrids. These types of experiments will be simplified by binding of the dye to short (5−6 base pair) duplexes. Molecular modeling experiments will also help determine the optimal sequence length for binding of the dye.

In addition, binding of the dye to PNA/RNA structures will be investigated. Comparison of NMR structures determined for PNA/RNA[17] and PNA/DNA duplexes[19] indicates that they have similar minor groove widths, so **DiSC$_2$(5)** should be readily bound by these hybrids.

Finally, analogues of **DiSC$_2$(5)** in which individual dye chromophores are covalently linked to one another should be even more effective ligands for PNA-containing hybrids as the entropic penalty for oligomerization of the dye and binding to the hybrid should be significantly reduced.

Conclusions. The cationic cyanine dye **DiSC$_2$(5)** binds with high affinity to a variety of PNA-containing hybrids. Binding causes a 114 nm hypsochromic shift in the absorption λ_{max}, resulting in an instantaneous color change from blue to purple. Circular dichroism, UV−vis, and thermal analysis indicate that the binding involves the spontaneous assembly of a helical aggregate of the dye, using the minor groove of the hybrid as a template to guide the assembly. This constitutes the first example of ligand binding to mixed sequence PNA-containing hybrids.

Experimental Section

Materials. HPLC-purified PNA oligomers were either a generous gift from Dr. Troels Koch of PNA Diagnostics A/S (Copenhagen, Denmark) or purchased from Perseptive Biosystems (Framingham, MA). Gel-filtration grade DNA oligomers were purchased from Midland Certified Reagent Company (Midland, TX) and used without further purification. **DiSC$_2$(5)**, **DiOC$_2$(5)**, and **DiSC$_{3+}$(5)** were purchased from Molecular Probes, Inc. (Eugene, OR) and used without further purification. **DiSC$_2$(3)** and **DiSC$_2$(7)** were purchased from Aldrich Chemical Co. (Milwaukee, WI) and used without further purification. **DiOC$_2$(7)** (laser dye grade) was purchased from Exciton (Dayton, OH) and used as received. Stock solutions of the PNA or DNA were prepared in 10 mM sodium phosphate buffer (pH 7.0). Concentrations were determined by absorbance at 260 nm with extinction coefficients calculated from DNA nearest neighbor values. For PNA, the absorbance was measured after incubating at 50 °C to disrupt the PNA secondary structure (ref 49). Stock solutions of cyanine dyes were prepared in methanol and filtered through glass wool. Concentrations were determined using the manufacturer's or literature extinction coefficients (given in methanol unless otherwise indicated): **DiSC$_2$(5)**, 260 000 M^{-1} cm^{-1} (651 nm); **DiOC$_2$(5)**, 238 000 M^{-1} cm^{-1} (579 nm); **DiOC$_2$(7)**, 254 000 M^{-1} cm^{-1} (687 nm in ethanol); **DiSC$_{3+}$(5)**, 160 000 M^{-1} cm^{-1} (653 nm); **DiSC$_2$(3)**, 180 000 M^{-1} cm^{-1} (554 nm);[68] **DiSC$_2$(7)**, 250 000 M^{-1} cm^{-1} (754 nm).[68]

Equipment. UV−vis measurements were performed on a Varian Cary3 spectrophotometer equipped with a thermoelectrically controlled multicell holder. CD measurements were recorded on a JASCO J-715 spectropolarimeter equipped with a thermoelectrically controlled single cell holder.

(64) The 114 nm shift of λ_{max} for **DiSC$_2$(5)**, while remarkable, is not without precedent for this dye. Shinkai and co-workers reported binding of the same dye to anionic polymers consisting of sugar/phenylboronic acid complexes linked to a helical polylysine. They reported analogous UV−vis shifts and induced CD exciton bands as we have observed, suggesting that the dye adopts similar aggregated structures in the two cases: Kimura, T.; Takeuchi, M.; Nagasaki, T.; Shinkai, S. *Tetrahedron Lett.* **1995**, *36*, 559−562.

(65) Elghanian, R.; Storhoff, J. J.; Mucic, R. C.; Letsinger, R. L.; Mirkin, C. A. *Science* **1997**, *277*, 1078−1081.

(66) Mucic, R. C.; Storhoff, J. J.; Mirkin, C. A.; Letsinger, R. L. *J. Am. Chem. Soc.* **1998**, *120*, 12674−12675.

(67) Storhoff, J. J.; Elghanian, R.; Mucic, R. C.; Mirkin, C. A.; Letsinger, R. L. *J. Am. Chem. Soc.* **1998**, *120*, 1959−1964.

(68) Sahyun, M. R. V.; Serpone, N. *J. Phys. Chem. A* **1997**, *101*, 9877−9883.

Hybridization. For spectroscopic experiments, equimolar mixtures of complementary strands were dissolved in a buffer containing 10 mM sodium phosphate (pH 7.0) and 100 mM NaCl. To minimize adsorption of the dye/PNA complexes to the walls of the cuvettes, 20% (v/v) methanol was also included in the buffer. (Where noted, only 10% methanol was used.) Samples were heated to 80 °C and then allowed to cool to room temperature over a period of ca. 1 h.

Dye Titrations. Samples were heated to 35 °C, and then a 2.0 μL aliquot of a 250 μM **DiSC$_2$(5)** stock solution was added. The sample was cooled to 15 °C and allowed to equilibrate for 5 min prior to recording the UV−vis or CD spectrum. The sample was then heated back to 35 °C prior to addition of the next aliquot.

Continuous Variations Experiment. Samples containing variable amounts of **DiSC$_2$(5)** and **PD2** (but a constant total concentration of 5.0 μM) were prepared in 10 mM sodium phosphate, 100 mM NaCl, and 10% methanol. Before addition of the dye, the sample temperature was raised to 35 °C. UV−vis absorbance spectra were recorded after equilibration at 15 °C, and the absorbance at 534 nm was plotted versus the mole fraction of dye.

Variable Temperature Spectroscopy. Samples were heated to 40 °C and equilibrated for 5 min prior to recording UV−vis or CD spectra. The temperature was decreased in 5 °C increments, and the samples were equilibrated for 5 min at each temperature prior to acquiring the spectrum.

Thermal Analysis. Unless otherwise indicated, samples were heated to either 65 °C (UV−vis experiment) or 40 °C (CD experiment) and equilibrated for 5 min. UV−vis absorbances at 260, 534, and 648 nm and CD intensities at 529 nm were recorded every 0.5 °C as the samples were cooled at a rate of 0.5 °C/min. T_m values were determined from the maxima of first-derivative plots. Normalized absorbances were calculated by dividing each curve by its lowest absorbance value. Fractional absorbances were calculated by the following formula:

$$\text{fractional absorbance} = (A_T - A_{min})/(A_{max} - A_{min})$$

where A_T is the absorbance at temperature T.

Microtiter Plate Assay for Hybridization. A 200 μL sample of buffer containing 10 mM sodium phosphate (pH 7.0), 100 mM NaCl, and 10% (v/v) methanol was added to each of eight wells in a microtiter plate. The desired amount of PNA and/or DNA (given in the caption to Figure 10) was then added to each well. **DiSC$_2$(5)** was then added to each well (15 μM final concentration), and the mixture was stirred with a pipet tip. The plate was then photographed using 35 mm color film. One exposure included a color calibration chart from Kodak to permit accurate reproduction of the sample colors during film development.

Appendix

Spectra recorded during the titration of **DiSC$_2$(5)** into **PD1** (Figure 1) were used for estimation of the binding constant. The difference spectrum obtained by subtracting the 4.5 μM dye spectrum from the 5 μM dye spectrum was divided by 0.5 μM, i.e., the concentration of added dye, to obtain the extinction coefficient spectrum for bound dye. (This calculation assumes that all of the dye added in that aliquot was actually bound to **PD1**. This assumption is verified by the observation that the difference spectra calculated after subsequent additions of the dye gave the same extinction coefficients.) This yielded $\epsilon_{534} = 117\,000\ M^{-1}\ cm^{-1}$ and $\epsilon_{648} = 39\,000\ M^{-1}\ cm^{-1}$ for bound dye. The corresponding values for the unbound dye are $\epsilon_{534} = 13\,000\ M^{-1}\ cm^{-1}$ and $\epsilon_{648} = 253\,000\ M^{-1}\ cm^{-1}$. These values were used in eq 2 to calculate the concentration of bound dye, where C_T, C_B, and C_f refer to the respective concentrations of total, bound, and free **DiSC$_2$(5)**.

$$A_\lambda = \epsilon_{\lambda,B}C_B + \epsilon_{\lambda,f}C_f = \epsilon_{\lambda,B}C_B + \epsilon_{\lambda,f}(C_T - C_B) \qquad (2)$$

Using the values for the extinction coefficients given above and $C_T = 5.0$ μM, the concentration of bound dye is 4.1 μM (using ϵ_{534} values) or 3.9 μM (using ϵ_{648} values), indicating that approximately 80% of the dye is bound under these conditions. Due to the stoichiometry of binding, 4.0 μM **DiSC$_2$(5)** will be bound to 0.67 μM **PD1**, leaving 4.33 μM **PD1** free.

$$K_B = \frac{0.67 \times 10^{-6}\ M}{(1.0 \times 10^{-6}\ M)^6(4.3 \times 10^{-6}\ M)} = 1.6 \times 10^{35}\ M^{-6}$$

Acknowledgment. This work was supported by a startup grant from Carnegie Mellon University. We are grateful to Dr. Troels Koch of PNA Diagnostics, A/S (Copenhagen, Denmark) for providing the PNA components of **PD2** and **PD3**. We thank Jennifer Seifert for measurement of the **DiSC$_2$(5)**/γ-cyclodextrin absorption spectrum. Photography was performed by Mr. Glenn Brookes of the CMU Photography and Graphic Services department. We also appreciate the helpful comments and suggestions of a reviewer.

Supporting Information Available: Figures showing the effect of **PD2** on UV−vis absorption spectra recorded for benzoxazole cyanine dyes and single base mismatch discrimination by **DiSC$_2$(5)** (PDF). This material is available free of charge via the Internet at http://pubs.acs.org.

JA9837553